Forming and spring-back simulation of CF-PEEK tape preforms

S. Cassola[1], M. Duhovic[1], L. Münch[2], D. Schommer[1], J. Weber[1], J. Schlimbach[1], J. Hausmann[1]

[1]Leibniz-Institut für Verbundwerkstoffe GmbH, Technische Universität Kaiserslautern, Erwin-Schrödinger-Straße 58, 67663 Kaiserslautern, Germany
[2]Institute of Aircraft Design, Universität Stuttgart, Pfaffenwaldring 31, 70569 Stuttgart, Germany

1 Introduction

The strive for high energy efficiency through lightweight design, especially for medium- and long haul aircrafts, has significantly increased the use of carbon fiber-reinforced plastics (CFRP) in the aviation industry in recent years [1]. High specific strength, corrosion resistance and improved fatigue life are only a few advantages that qualify CFRPs as structural parts in aircrafts. However, high material, manufacturing and assembly costs are still restricting their use [2]. Highly automated manufacturing processes, which provide a high degree of mounting part integration are needed to lower the part and assembly costs. Structural frames in aircraft fuselages currently make use of a differential design and consist either of aluminum, which provides insufficient specific strength or carbon fiber-reinforced thermosets, which involve long processing times. To overcome these drawbacks, a carbon fiber-reinforced, thermoplastic frame with integrated mounting parts has been developed in order to reduce the complexity of the assembly process. The frame is manufactured in an one-shot process involving tape preform production by automated tape laying (ATL) and a subsequent thermoforming step. ATL allows near-net-shape manufacturing of preforms, which reduces scrap rates to a minimum [3]. The subsequent thermoforming step enables the production of complex 3D-parts with low cycle time [4].

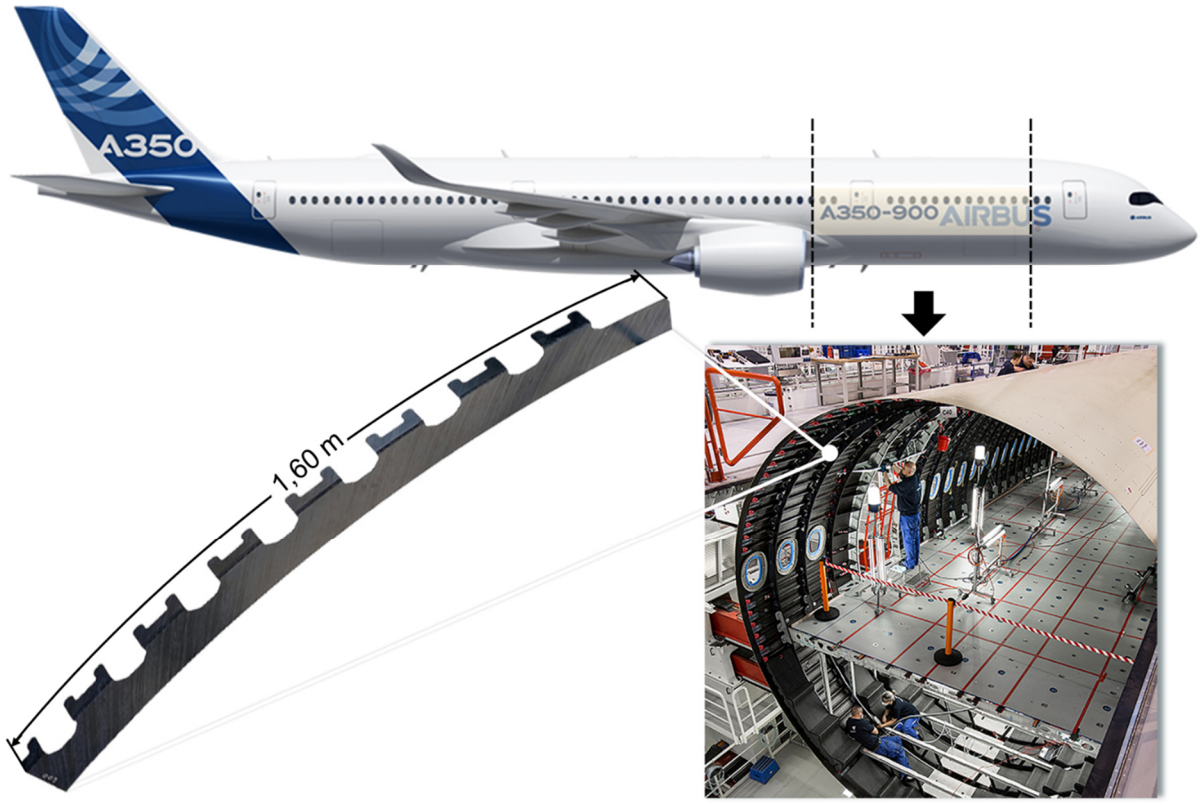

Fig. 1: Location of the integral structural frame within an Airbus A350 fuselage (images courtesy of Airbus, Premium Aerotec and Leibniz-Institut für Verbundwerkstoffe).

During thermoforming, the fiber orientation has an impact on drapability and the formation of wrinkling, while in the final part, the fiber orientation influences local and overall mechanical properties [5]. Hence,

information about the fiber orientation in the tape preform during thermoforming and in the final part is of high importance. Here, a finite element based thermoforming simulation can provide useful knowledge about the final fiber orientation and the possibility of manufacturing defects occurring such as wrinkling. However, such simulations of tape preforms are a particular challenge compared to organosheets with woven reinforcement structures due to the following complexities:

- Multiple layers (e.g. 14 or more) of thermoplastic tape material is laid-up in various, customized directions and sometimes also along curved paths to build up the laminate
- The thickness of the laminate is not necessarily constant and various ply drop-off zones within the laminate may also exist
- Simulations must be non-isothermal and consider temperature dependent material properties in the case of both, the thermoforming and spring-back stages

Based on the idea of Sidhu et al. [6], who combined shell and truss elements within a unit-cell, Duhovic et al. [7] developed a forming simulation method to predict the resulting fiber orientation and the influence of stiches on a dry textile reinforced structure. Schommer et al. [5] further developed this approach so that non-isothermal thermoforming processes can be accurately modelled by taking into account the temperature dependent viscosity of the thermoplastic resin. This work presents a simulation approach that allows accurate modelling of the thermoforming process of tape preforms using the example of the integral aircraft fuselage frame, shown in Figure 1. Furthermore, a spring-back simulation is carried out from the final state of the forming simulation, which takes into account fiber orientations, the residual stresses and strains. In the following sections, the necessary material characterization tests, the model calibration, the build-up of the demonstrator thermoforming simulation and finally the spring-back simulation are described.

2 Material characterization

To be able to develop an accurate thermoforming and spring-back simulation, the material needs to be characterized. One of the dominating deformation modes during thermoforming is bending [4]. The bending behavior at high temperatures is mostly determined by the fibers and is also influenced by the strain rate and temperature dependency of the polymer. A three-point bending test at elevated temperature is carried out in order to measure the bending stiffness. Another important influence on the forming behavior is given by the in-plane shearing of the preform [4]. In contrast to bending, the overall shear behavior is even more sensitive to the temperature dependency of the matrix material as well as on fabric shearing. Horizontal picture frame testing at elevated temperatures is an appropriate way to determine the shear properties of thermoplastic preforms. The specimen is first heated to a constant temperature in an expected forming temperature range and then deformed in in-plane shear. The material that has been characterized in this work is a carbon fiber reinforced poly-ether-ether-ketone (PEEK), which is produced by CYTEC (CYTEC APC-2-PEEK). In the following sections, the material characterization procedures are explained in more detail.

2.1 Three-point bending test

The three-point-bending tests are performed on an Eplexor Dynamic Mechanical Thermal Analysis (DMTA) testing machine with a maximum load range of ±150 N. The CYTEC APC-2-PEEK material is tested on 0° UD specimens with 15 layers (thickness ≈ 2 mm) at a testing speed of 1 mm/min. The testing procedure is based on the description of the DIN EN ISO 14125 standard for fiber reinforced materials. The specimens are heated to process temperature in a heating chamber to ensure a homogeneous temperature and deformed after a defined waiting time. For each combination of temperature and material, 5 measurements are carried out. Experiments are performed at 360 °C, 380 °C and 400 °C for fully and partially consolidated laminates. Full consolidation of the specimens is achieved by an additional pressing process after tape-laying in order to eliminate any potential voids in the laminate. Figure 2 shows the experimental setup (top), the comparison of the bending behavior at 360 °C, 380 °C and 400 °C (bottom, left) and the three-point bending test results for both, fully and partially consolidated specimens (bottom, right).

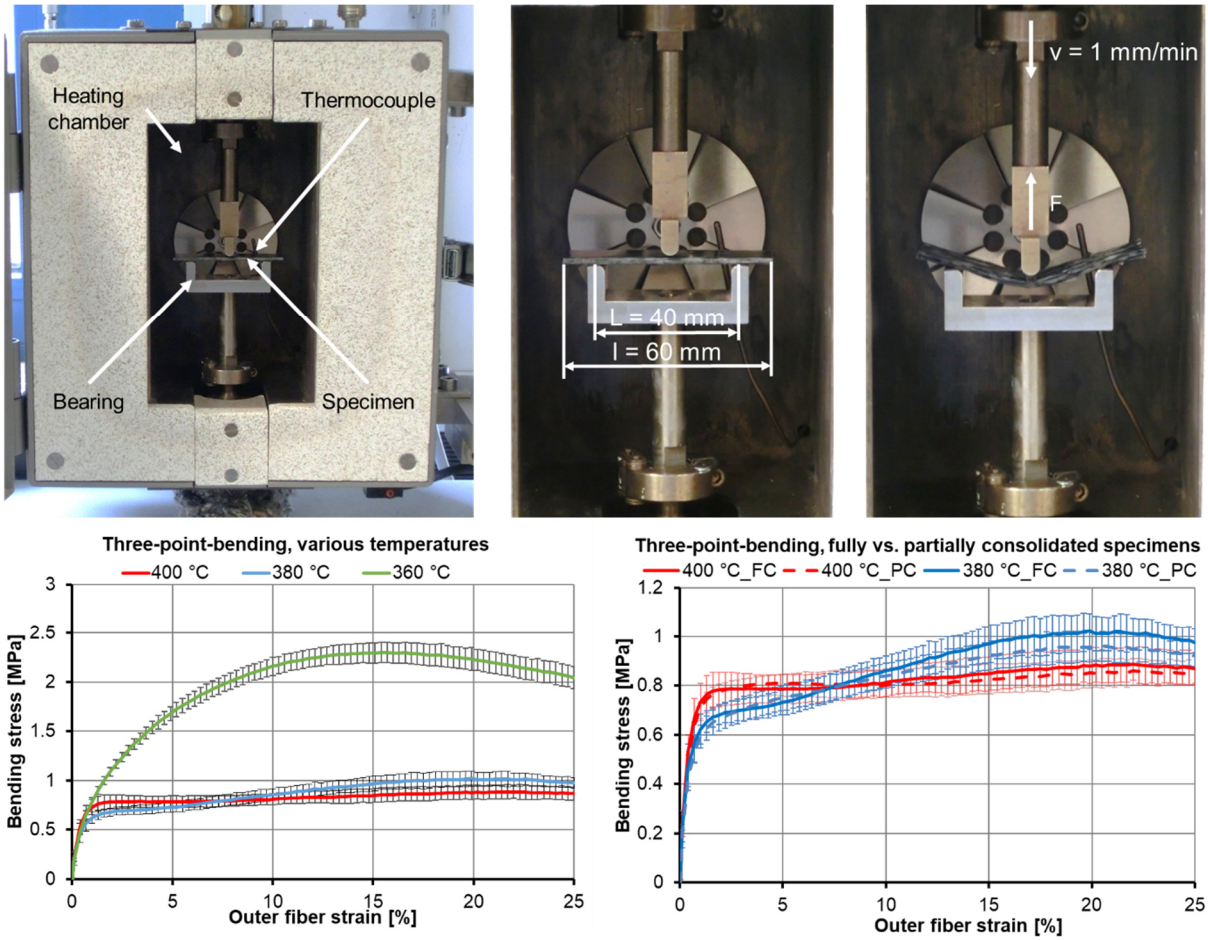

Fig. 2: Experimental setup of the three-point-bending test (top), mean values of the three-point bending test at 360 °C, 380 °C and 400 °C (bottom, left) and results of the three-point bending test for fully consolidated (FC) and partially consolidated (PC) specimens (bottom right).

A clear drop in bending resistance between 360 °C and 380 °C can be observed (Figure 2, bottom left), whereas there is no significant difference between 380 °C and 400 °C. Testing at 360 °C is close to the melting point of PEEK at 343 °C, resulting in a greater contribution from the matrix to the bending resistance via its viscosity and inter-fiber shearing. At higher temperatures, the PEEK material is fully molten and reaches a minimum viscosity, so that the overall bending behavior is mainly determined by the bending stiffness of fibers and becomes relatively temperature independent. No significant differences were found between the fully and partially consolidated specimens in the results of the three-point bending test. The variations were within the standard deviation of the individual specimens.

2.2 Picture frame test

Picture frame testing at elevated temperature is carried out on a specialized stand-alone test-bench, which was developed in-house at the Leibniz-Institut für Verbundwerkstoffe (IVW). The test-bench consists of a horizontally mounted zwickiLine Z2.5 TN+ 2.5 kN material testing machine allowing maximum test speeds of up to 3000 mm/min. The heat source is provided by two Watlow Raymax 1120RM-24 heating elements that achieve a homogeneous heating distribution (of up to 400 °C) on the top and bottom surfaces of the specimen. The distance of the top and bottom heating panel to the specimen can be adjusted. Additionally, the top panel slides away allowing quick and safe access to the specimen. A thermal camera and two thermocouples are used to monitor the temperature. The shear behavior of the CYTEC APC-2 PEEK material is tested on specimens with a $[0°/90°/0°/90°/0°/90°/0°/90°]_S$ lay-up sequence. As a consequence of the bending tests, shear tests are only conducted at 380 °C, which proved to be sufficient to ensure a fully molten thermoplastic matrix. Analogous to the three-point-bending tests, partially and fully consolidated specimens are tested at a test speed of 100 mm/min. Figure 3 shows the test-bench, a fully deformed specimen clamped in the picture frame, an image from the thermal camera and the resulting force vs. shear angle curve for partially and fully consolidated specimens at 380 °C.

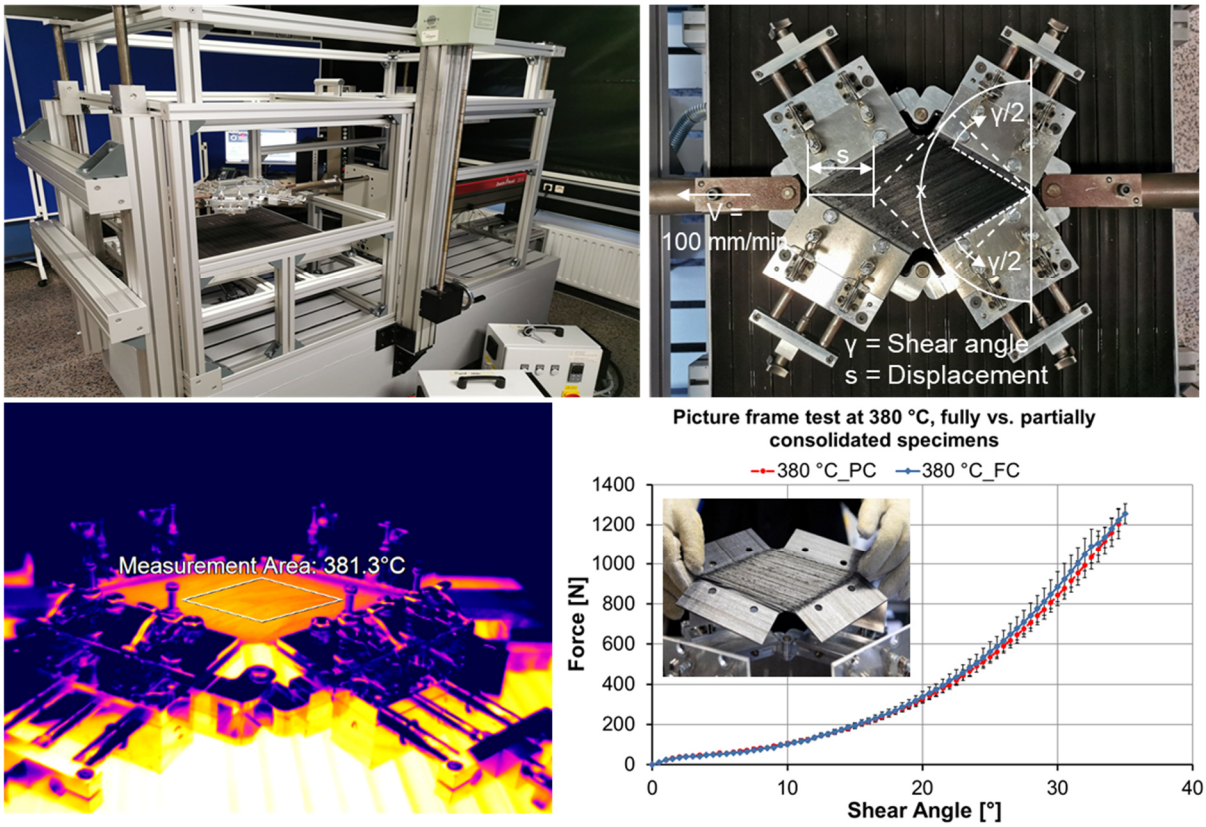

Fig. 3: Test-bench for picture frame testing (top, left), picture frame with fully deformed specimen and schematic of the displacement (top, right), thermal camera image (bottom, left) and resulting force vs. shear angle curve for partially (PC) and fully consolidated (FC) specimens (bottom, right).

Similar to the bending tests, there is a negligible influence of the degree of consolidation on the shear behavior. Thus the average of the two curves shown in Figure 3 (bottom, right) are used as a reference for the picture frame test simulation which is described in Section 3.2. However, small differences in surface structure and specimen thickness during heating between the partially and fully consolidation specimens were detected. This effect may be due to the different states of residual stresses in the specimen, which are reduced as soon as the matrix melts and no longer contributes to additional stresses in the fibers.

3 Forming Simulation

3.1 Material model

The material model for the simulation is based on the unit-cell approach developed by Duhovic et al. [7] and Schommer et al. [5]. Here, the behavior of the material is not described by a single element, but by a combination of 1D and 2D finite elements. The interaction of all the elements within the unit-cell describes the real behavior of a repeating structure of the organosheet or tape preform. For this purpose, one layer of shell elements and one layer of beam elements are used per layer of tape. The beam elements describe the fiber orientation as well as the bending properties of the tape, while the shell elements simulate the shear behavior. A second layer of shell elements without mechanical properties is also created, sharing nodes with the beam elements, to allow thermal contact between shell and beam elements. Figure 4 shows a lay-up sequence of 13 layers of tape and the schematic representation of the unit-cell. This approach allows the forming simulation of organosheets and tape preforms without the use of user-defined subroutines in LS-DYNA®.

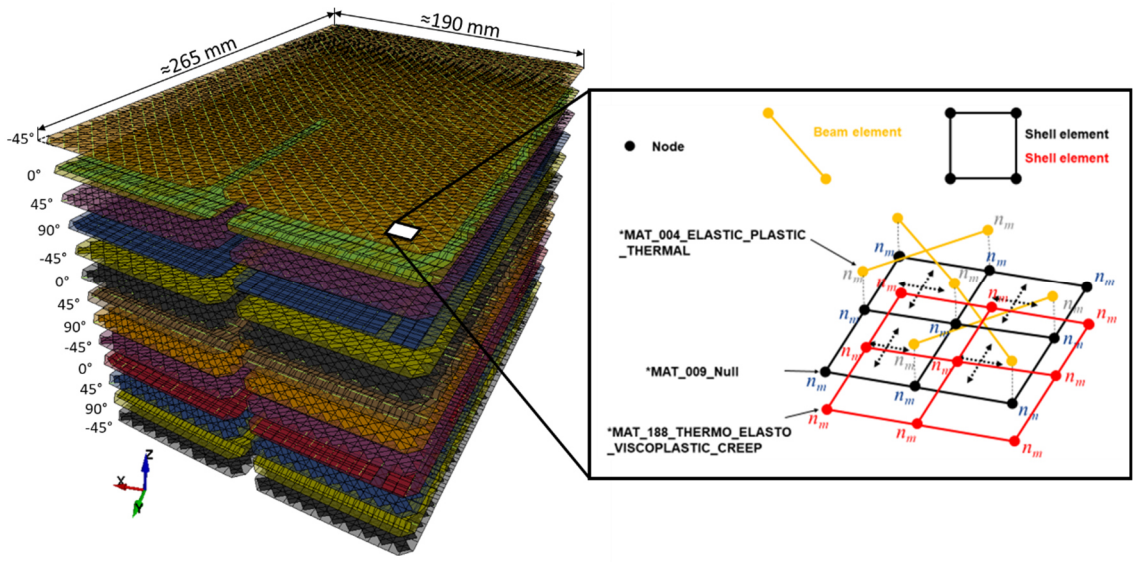

Fig. 4: Lay-up sequence of 13 layers of tape and schematic representation of a unit-cell in relation to the size of the model.

3.2 Calibration of the material model

To fit the bending and shear behavior of the simulation model to the behavior of the specimens, both, the bending and shear characterization tests are simulated. From the experimental results, an initial estimate of the material properties is obtained, which is adjusted in subsequent simulations in order to calibrate the behavior of the unit-cell. The bending properties are adjusted first, since no shear forces are generated during the bending test. The fitting parameters for the bending simulation are the tensile modulus, the hardening modulus and the yield stress of the fibers, which can be set in the **`*MAT_004_ELASTIC_PLASTIC_THERMAL`** keyword card. The bending properties are assumed to be isothermal. An automated fitting process, using the optimization capabilities of LS-OPT®, is developed in order to determine the appropriate value for the hardening modulus and the yield stress, whereas the tensile modulus is fitted manually. Because the simulation time step depends on the tensile modulus, it is possible to balance the beam cross-sectional area and the tensile stiffness in order to maintain the same overall stiffness but achieve a reasonably high time step. Figure 5 illustrates a bending specimen (top, left) and the corresponding simulation model (top, right) as well as the results before (bottom, left) and after (bottom, right) parameter fitting of the simulated and the experimental three-point bending.

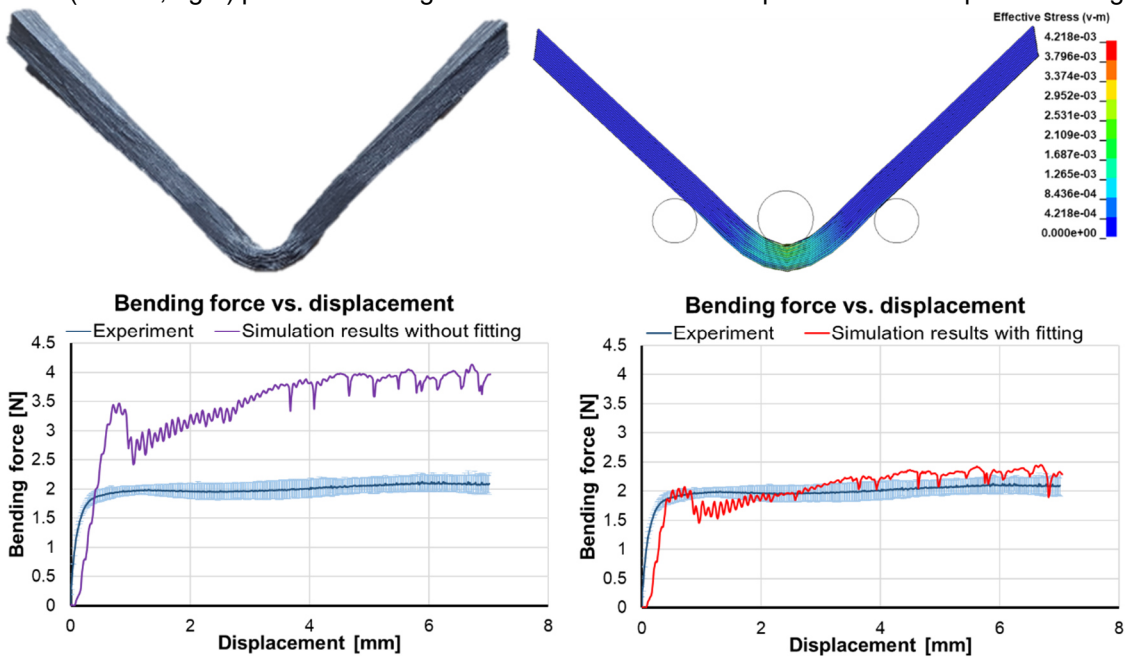

Fig. 5: 3-point-bending test specimen (top, left) and simulation model (top, right), simulation results before (bottom, left) and after (bottom, right) adjustment of the bending properties for 400 °C.

Since the bending test at 1 mm/min takes about 7 minutes, a high speed up factor of 1000x needs to be used for the simulation in order to achieve reasonable simulation times. The oscillating force in the simulation of the bending test is due to the size of the unit-cell, which is designed to fit the final part model and is therefore too coarse for the bending specimen and due to the high simulation velocity. Using a finer resolution and a lower speed up factor improves the results while increasing the computational cost significantly.

Similarly to the bending properties of the beam elements, the shell elements are fitted in a picture frame test simulation. LS-OPT® is used to fit the stress-strain-curve of the shell elements, which represent the shearing and are described by **`*MAT_188_THERMO_ELASTO_VISCOPLASTIC_CREEP.`** For this purpose a pre-processor stage is created in LS-OPT® that utilizes the 'user-defined' command in combination with a Python script. A text file containing six supporting parameters is passed to the Python script, which subsequently calculates a hermetic spline function that approximates the stress-strain-curve. The stress-strain-values of the spline function are written in an LS-DYNA® include file and passed to the next stage that carries out the simulation. The six supporting points of the hermetic spline function were used as the optimization parameters. Figure 6 shows the sheared specimen (top, left) and simulation model (top, right) as well as the simulation results before and after parameter fitting.

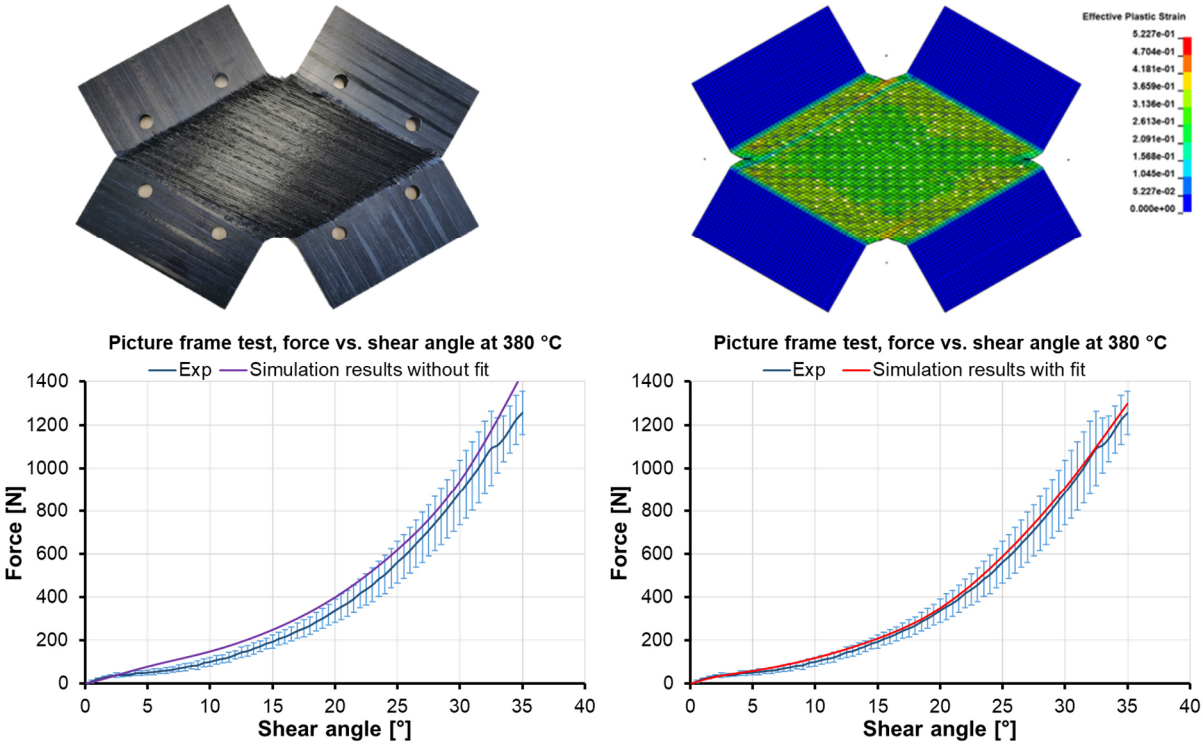

Fig. 6: Sheared specimen (top, left), sheared simulation model (top, right), simulated picture frame test results before (bottom, left) and after (bottom, right) parameter fitting.

Since the dimensions of the shear specimen are within the order of magnitude of the final part, no negative effects of the mesh resolution can be observed in the simulation results. Furthermore the picture frame test is carried out at 100 mm/min and therefore, takes only 40 seconds which allows for a reasonable computation time at lower speed up factors.

3.3 Build-up of the demonstrator simulation

An aircraft fuselage integral frame, which is manufactured by thermoforming a thermoplastic tape preform, serves as a demonstrator geometry for the simulation. The simulation is composed of unit-cells, in which the beam elements are generated based on the machine paths of the tape laying robot. After creating the whole demonstrator model, the simulation contains about 1.2 million elements. Each of the 13 layers of tape is represented by one layer of unit-cells. The individual layers of unit-cells are connected by **`*CONTACT_AUTOMATIC_SURFACE_TO_SURFACE_TIEBREAK_THERMAL`** using option 4 to allow tangential motion with frictional sliding. The maximum characteristic element size in this nearly

homogeneous mesh, is 6.15 mm with an average edge length of 6 mm. In areas that come into contact with the radii of the tooling, the elements are divided in half in radial direction in order to represent the geometry adequately and thus preventing penetration of the individual layers in the simulation. Due to the only locally refined mesh, it is possible that the forming simulation can be solved in under 10 hours on a desktop PC. The preform is held in position using beam elements, which deform according to the blank holder forces in the forming process. Figure 7 shows the suspended preform between the press tooling and the final geometry with an exploded view of the resulting fiber orientation represented as beam elements. The fiber orientation information together with the resulting stresses and strains are passed on to the warpage and distortion simulation, which allows calculation of the spring-back effect. Following the spring-back simulation, the beam elements can also be used to transfer the fiber orientation information on to further structural or crash simulation models. To map the fiber orientation to subsequent simulations, a mapping tool like ENVYO® or the IVW proprietary tool described in [8] can be used.

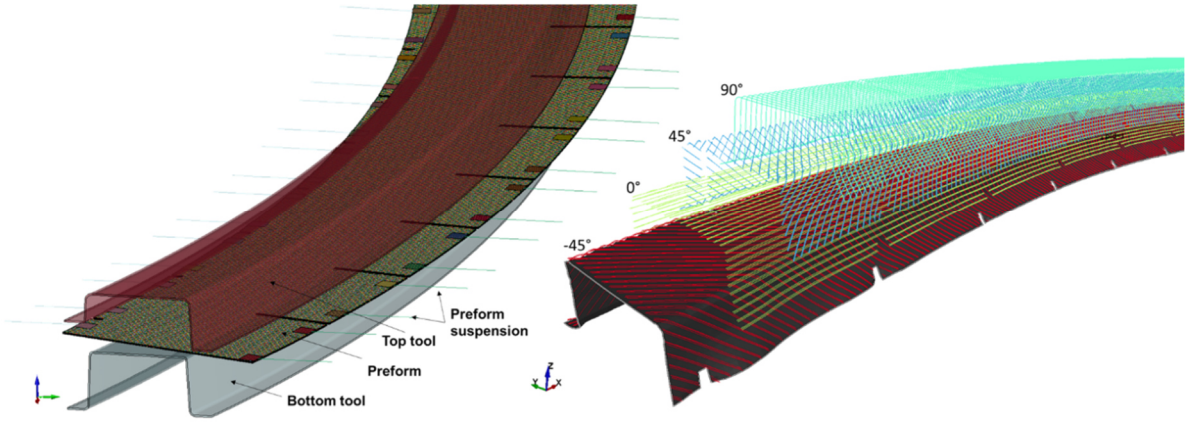

Fig. 7: Preform inserted in press tooling (left) and exploded view of the final fiber orientation after thermoforming (right).

Figure 8 shows the non-isothermal thermoforming process of the aircraft fuselage. It can be seen that the preform, which is heated to 400 °C, rapidly cools down as soon as it comes into contact with the pressing tool that has a temperature of 277 °C. Non-isothermal thermoforming simulation utilizing the unit-cell approach is considered to be an appropriate solution to model the temperature-dependent bending and shear behavior without user-defined subroutines. However, the current model assumes constant coefficients of friction over temperature between layers and between tooling and preform, which is seen to be inaccurate and a potential area for improvement.

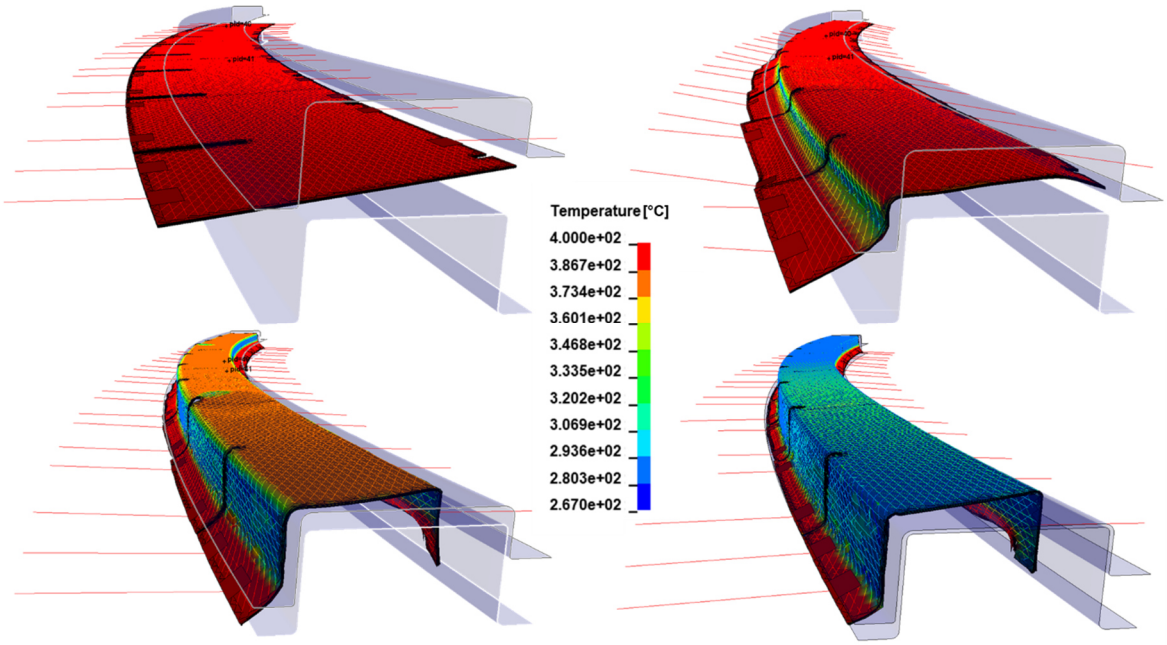

Fig. 8: Non-isothermal thermoforming process simulation of the aircraft fuselage integral frame.

4 Spring-back simulation

Generally, a spring-back simulation can be enabled by defining a part set within the ***INTERFACE_SPRINGBACK_LSDYNA** keyword card. A “dynain”-file will be automatically created containing information about residual stresses from the forming operation. Subsequently the “dynain”-file needs to be included together with the separate input deck created for the spring-back simulation. For this work, the part set consists of all shell and beam elements so that the “dynain”-file contains information about residual stresses within the matrix and in the fibers.

4.1 Picture frame samples

Initially, a spring-back or warpage/distortion simulation is carried out for the picture frame test specimens. As a measurement reference for the simulation, the hole spacing in the cooled sample in its deformed state are compared with the spacing of the pins in the picture frame. For the spring-back simulation, the thermal expansion coefficient of the shell elements is set to be the temperature-dependent thermal expansion coefficient of PEEK [9]. The thermal expansion coefficient of the beam elements corresponds to the longitudinal coefficient of expansion of the composite material as specified by the material data sheet. Figure 9 shows the measured reference directions on a picture frame specimen and the resulting deformation calculated by the spring-back simulation.

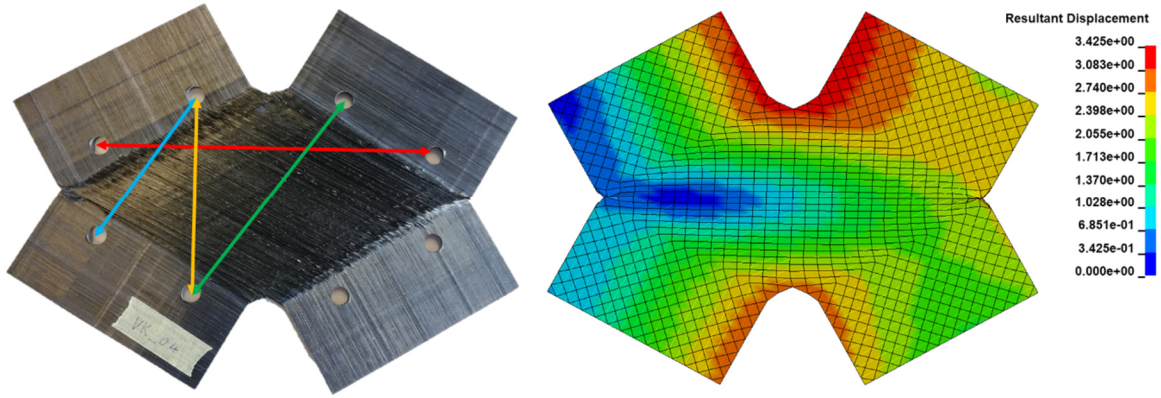

Fig. 9: Distance over which the warpage/distortion of the specimen was determined based on a picture frame specimen (left). Spring-back simulation with resulting deformation of the specimen (right).

In comparison to the experimental results, the result of the distortion in the simulation underpredicts the experimental results in the vertical and diagonal directions (Figure 9 left, yellow, green and blue line) while it overestimates the deformation of the specimen in the pulling direction (Figure 9 left, red line) of the picture frame test. Table 1 shows a comparison of the measured results and the spring-back simulation. The spring-back simulation clearly shows the correct direction and overall tendency of the warpage behavior with only small deviations from the experimental results. However, further optimization can be achieved through parameter studies to determine the dominant parameters and improve prediction accuracy.

	Simulation	**Experiment**
Vertical *(Figure 9 left, yellow line)*	4.1 %	5.3 % ± 1.7 %
Horizontal – pulling direction *(Figure 9 left, red line)*	-1.2 %	-0.3 % ± 0.8 %
Diagonal long *(Figure 9 left, green line)*	2.6 %	3.8 % ± 0.9 %
Diagonal short *(Figure 9 left, blue line)*	1.4 %	4.9 % ± 1.3 %

Table 1: Comparison of the warpage/distortion measured in the deformed picture frame specimens vs. spring-back simulation.

4.2 Aircraft fuselage integral frame

The spring-back simulation is also performed for the aircraft fuselage integral frame demonstrator. Figure 10 shows the deformation of the frame resulting from spring-back and the predicted angles

between the top and the sides of the frame. Although the simulation predicts the correct direction and tendency of the spring-back behavior, consistent predictions to within 1° accuracy of the experimental measurements remains a challenge.

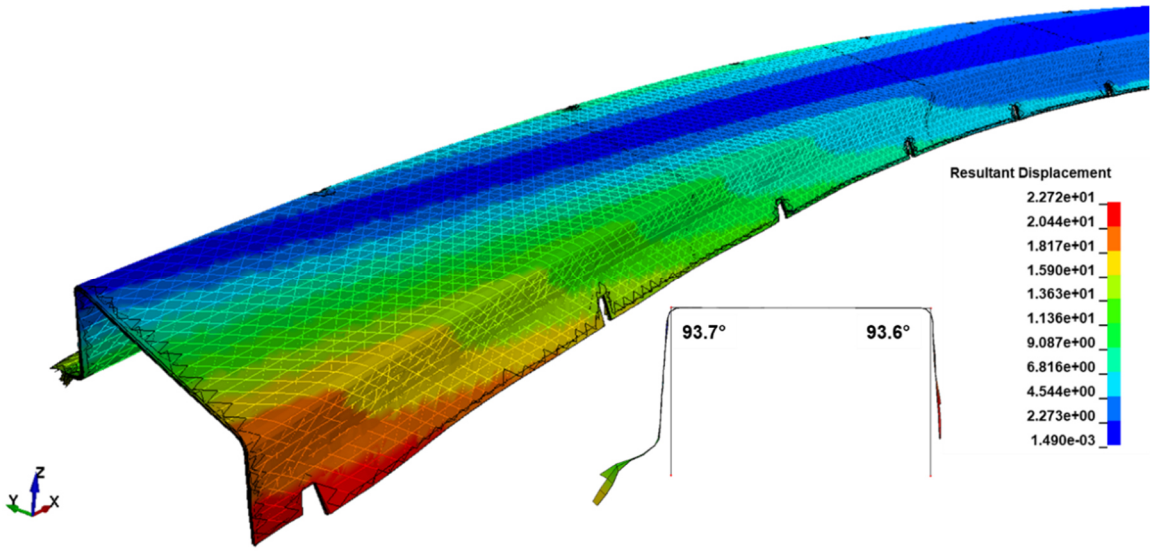

Fig. 10: Spring-back simulation displacements and predicted angles between top and sides of the integral frame demonstrator.

For a comparison between the real and simulated fiber orientation in the frame, fiber orientation angles are measured at 5 locations across the full width of the part and 4 times at areas with cut-outs. The measurement areas are shown in Figure 11 (top and bottom, right) together with a comparison of the measured fiber orientation (bottom, left) in the frame and in the simulation model. Values are averaged over the 15 measurement areas along the length of the part for each of the 5 (4) positions across the width. A close to constant offset (average ≈ -2.8°) can be observed between the measured and simulated fiber orientation angles. It is suspected that this is due to differences between the coefficients of friction used in the simulation and the real (temperature-dependent) friction between the tool and preform as well as friction between individual layers.

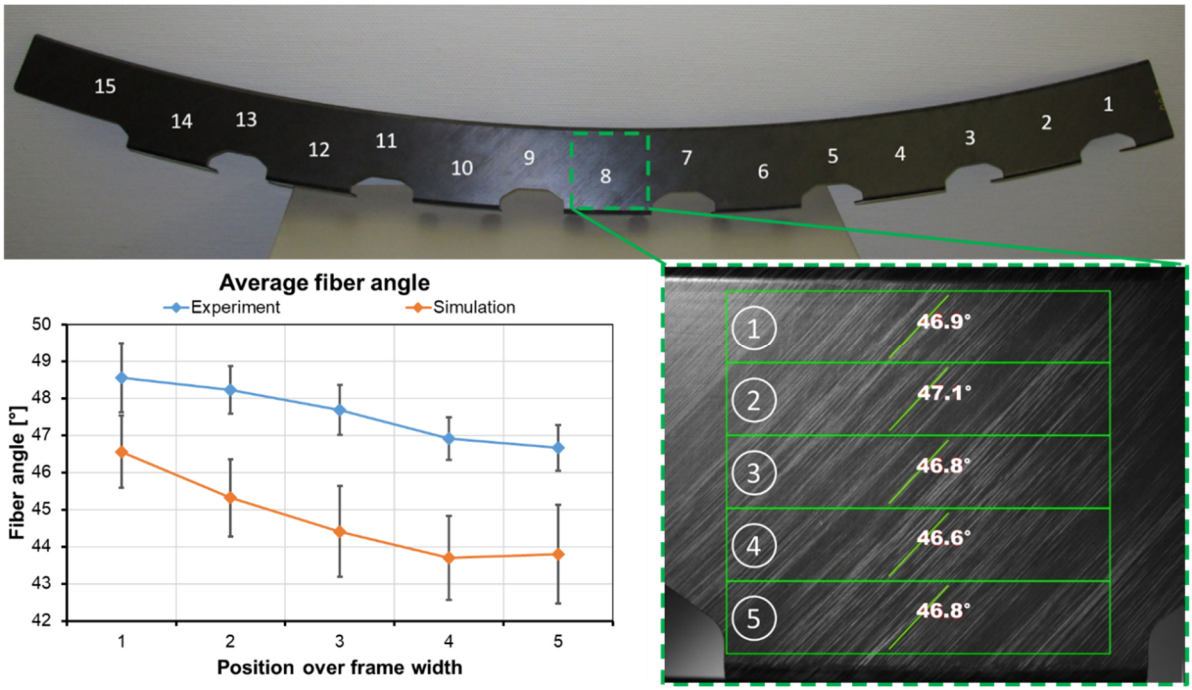

Fig. 11: Measurement areas (top and bottom, right) and comparison of measured and simulated fiber orientation angles (bottom, left).

The spring-back simulation based on the mesh of the thermoforming simulation is considered to be an appropriate solution to couple forming and spring-back simulations. However, further adjustments and calibration of the spring-back parameters in the simulation is required. One important aspect that needs to be taken into account in the evaluation of the results is the dependency of the cooling rate. Hence, effects such as varying shrinkage/spring-back due to different degrees of crystallization have not been implemented in the current simulation models. The spring-back simulation model at present can therefore only be adapted for one specific material cooling rate.

5 Summary

The principle of the combined element unit-cell modelling approach allows the representation of temperature-dependent bending and shear behavior of the individual tape layers to be simulated at the component level. Each layer of tape is modelled by beams describing the bending properties of the fibers, a layer of shells describing the shearing behavior of the fibers and thermoplastic matrix and an additional thermal layer of shells sharing nodes with the beams, thus allowing thermal contact between beams (fibers) and shells (matrix). Each layer of the preform can be modelled individually and directly from the machine paths of the tape laying robot, closing the gap between simulated preform production and thermoforming simulations. A change of the fiber orientation is allowed via sliding of the individual layers over one another during forming. The simulation results showed an average offset in prediction of the fiber orientation at different areas of the frame of around -2.8°. Resulting fiber orientations can be mapped to subsequent structural or crash simulations enabling a consistent CAE process chain. A spring-back simulation using fiber orientation, stress and strain information resulting from the thermoforming simulation has been performed and has proved to be a suitable tool to predict overall tendencies for part distortions due to cooling.

6 Acknowledgement

The authors would like to thank the project partners *Premium Aerotec GmbH*, *Automotive Center Südwestfalen*, *Fraunhofer Institute for Casting, Composite and Processing Technology IGCV* and the *Fraunhofer Institute for Manufacturing Technology and Advanced Materials IFAM* for their help and support during the course of that project. Furthermore we would like to thank the *Faserinstitut Bremen e.V.* for providing the fiber orientation measurements.

7 Literature

[1] Bachmann, J.; Hidalgo, C. and Bricout, S.: Environmental analysis of innovative sustainable composites with potential use in aviation sector—A life cycle assessment review, Science China Technologal Science, 60, no. 9, 2017, pp. 1301 – 1317.

[2] Soutis, C.: Carbon fiber reinforced plastics in aircraft construction, Materials Science and Engineering A, 412, no. 1–2, 2005, pp. 171 – 176.

[3] Kropka, M.; Muehlbacher, M.; Neumeyer, T. and Altstaedt, V.: From UD-tape to Final Part – A Comprehensive Approach Towards Thermoplastic Composites, Procedia CIRP, 66, pp. 96 – 100, 2017.

[4] Akkerman, R.; and Haanappel, S. P.: Thermoplastic composites manufacturing by thermoforming, Advances in Composites Manufacturing and Process Design, 2015, pp. 111-129.

[5] Schommer, D.; Duhovic, M. and Hausmann, J.: Modeling non-isothermal thermoforming of fabric- reinforced thermoplastic composites, 10th European LS-DYNA Conference 2015, Würzburg, Germany.

[6] Sidhu, R. M. J. S.; Averill, R. C.; Riaz, M. and Pourboghrat, F.: Finite element analysis of textile composite preforms stamping, Composite Structures, 52, no. 3 – 4, 2001, pp. 483 – 497.

[7] Duhovic, M.; Mitschang, P.; and Bhattacharyya, D.: Modelling approach for the prediction of stitch influence during woven fabric draping, Composite Part A, Applied Science and Manufacturing, 42, no. 8, 2011, pp. 968 – 978.

[8] Duhovic, M.; Patil, P.; Scheliga, D.; Schommer, D.; Münch, L. and Hausmann, J.: Development of a Customized Beam-to-Shell Element Model Mapping Tool, 12th European LS-DYNA Conference 2019, Koblenz, Germany.

[9] Ehrenstein, G. W.; Riedel, G. and Trawiel, P.: Thermal analysis of plastics, Carl Hanser Verlag GmbH & Co. KG, ISBN: 978-3-446-43414-1, 2004.